H_3PO_4-based wet chemical etching for recovery of dry-etched GaN surfaces

Sabria Benrabah[1,2,4], Maxime Legallais[2], Pascal Besson[3], Simon Ruel[1], Laura Vauche[1], Bernard Pelissier[2], Chloé Thieuleux[4], Bassem Salem[2], Matthew Charles[1]

1. Univ. Grenoble-Alpes, CEA, LETI, 38000 Grenoble, France

2. Univ. Grenoble-Alpes, CNRS, CEA-LETI, Grenoble INP, LTM, F-38054 Grenoble, France

3. STMicroelectronics, Crolles Cedex, 38920, France

4. Laboratory of Catalysis, Polymerisation, Processes and Materials, C2P2 UMR 5128 CNRS-UCB Lyon 1-CPE Lyon, Université de Lyon, Institut de Chimie de Lyon, CPE Lyon 43 Bvd du 11 Novembre 1918, F-69616 Villeurbanne, France

Abstract

The impact of several wet etchants commonly encountered in the microelectronic industry on the surface chemistry of GaN on silicon was explored. In order to get closer to fully recessed gate HEMT fabrication processes, we investigated different kinds of GaN surfaces. This study was conducted on as-grown GaN and dry etched GaN, with etching consisting of inductive coupled plasma reactive ion etching (ICP-RIE), followed by atomic layer etching (ALE) and O_2 plasma stripping. The impact of each wet treatment was evaluated by parallel Angle Resolved X-ray Photoelectron Spectroscopy (pAR-XPS). Treatment with phosphoric acid (H_3PO_4) showed a significant modification of the surface and further studies were performed using this treatment. The impact of H_3PO_4 on GaN surface chemistry and morphology was assessed by pAR-XPS and atomic force microscopy (AFM) respectively. A delayed effect was observed for dry etched samples compared to as-grown samples, with a successful recovery of the surface after 60 minutes of treatment. We also proposed a mechanism explaining the progressive formation on steps on the surface over time. Further research was performed on dry etched samples without ALE which also modified the delay time of the H_3PO_4 treatment, but still enabled a recovery of the surface morphology. In contrast to other studies, we showed that, with the appropriate choice of parameters for the H_3PO_4 treatment, it was possible to successfully recover the GaN surface after dry etching without significantly opening dislocation holes. This is therefore a promising treatment to be used during GaN HEMT processing to recover good quality surfaces after etching.

1. Introduction

Gallium nitride (GaN) has attracted significant interest due to its intrinsic properties and potential applications in microelectronics. GaN is a direct wide bandgap material that presents exceptional properties for next-generation power electronic devices. With a high saturation velocity and a high operating voltage, GaN-based devices can operate at high frequency and with excellent efficiency, making GaN a material of choice in power applications.

Unlike other semiconductors such as GaAs, SiC or Si, GaN substrates are very expensive and only available in small diameters. This means that growth on these substrates is prohibitively expensive to compete with silicon or SiC for power applications. Instead the growth of GaN is typically performed

on a foreign substrate such as Si, sapphire or SiC [1] using molecular beam epitaxy (MBE) or Metal Organic Chemical Vapour Deposition (MOCVD). In particular, growing GaN on silicon has several advantages: it reduces the cost due to large diameter (200 mm) substrates and allows compatibility with large silicon fabrication plants [2]. However, growing on a different substrate has also disadvantages due to lattice mismatch and differences in thermal expansion coefficients. These can lead to point-defects and extended-defects [3] such as dislocations. As a result, many studies have been performed to find a reliable and efficient method to investigate surface defects and dislocations in GaN. A popular method to evaluate surface defects is the use of wet-chemical etching. Hot phosphoric acid (H_3PO_4) and molten potassium hydroxide (KOH) have been demonstrated to etch pits at dislocations on c-plane GaN [4], making them easier to count reliably.

In this study, we will concentrate on surface defects rather than dislocations. Unlike bulk materials, the chemistry and physics of the surface are different due to undersaturated coordination configurations which lead to dangling bonds and adsorption of contaminants such as oxygen and carbon. These adsorbates are also responsible for some issues in GaN-based transistors as they can trap charges and thus impact MOS interface trap density, dielectric quality, transistor threshold voltage shift and channel mobility [5]. Hence, techniques to avoid contamination and methods to prepare a very clean surface are very important. Many cleaning/etching studies were performed on GaN wafers. Atomic Layer Etching (ALE) or Inductively Coupled Plasma Reactive Ion Etching (ICP RIE) dry etching techniques are based on the use of a plasma [6]. However, energetic ions damage the GaN surface. Electrical properties are then degraded [7] because of an increase of the interface state density [8] [9], an increase of the 2 Dimensional Electron Gas (2DEG) sheet resistance [10] and a lowering of the electron mobility [9]. *Ruel et al*. [11] reported that an ALE final step after an ICP-RIE process reduced the impact on sheet resistance, but damages induced by the process were not fully removed. In contrast, an inexpensive wet etching produces negligible damage and generally results in smoother surfaces. It is also a good technique to remove damages induced by dry etching processes [12] [13].

However, c-plane GaN is known for its inertness toward wet chemical etchants [14]. Among all the conventional wet etching treatments, only high boiling point chemicals result in significant modifications. There is therefore a need to better understand the chemistry and physical properties of the GaN surface in order to control them and facilitate GaN based transistor manufacturing.

As stated above, H_3PO_4 and KOH result in morphological modifications and are accurate means of revealing surface defects. They also significantly modify the surface chemistry, with water and hydroxyl adsorption [15], but also a considerable amount of carbon addition [16]. Many studies were conducted on epitaxial GaN films grown by HVPE on sapphire, as the objective was to reveal and more easily count dislocations. *Xu et al.* [17] studied the effect of H_3PO_4 on GaN grown by different techniques and on different substrates.

The current article thus focuses on the surface modifications induced by wet treatments on MOCVD grown GaN on silicon. Parallel Angle Resolved X-ray Photoelectron Spectroscopy pAR-(XPS) and Atomic Force Microscopy (AFM) were used to that end. We have investigated ex-situ wet chemistries based on commonly used solutions in the microelectronic industry and reported in the literature. In the first part, we will examine their impact on as-grown GaN before performing an in-depth study of the H_3PO_4 wet etching of as-grown GaN and dry-etched GaN, to be closer to the transistor manufacturing process.

2. Material and methods

GaN layers were grown by MOCVD (Metal Organic Chemical Vapour Deposition) on 200 mm diameter silicon (111) substrates. More details about the growth protocol used can be found in [18]. The GaN layers were c-plane, with a gallium polarity. Unintentionally doped GaN was used for the initial part of the work, followed by intentionally silicon-doped n-type GaN with a carrier concentration of $5x10^{17}$ cm^{-3}. This lightly doped material was chosen to aid the fabrication of simple electrical test structures (not reported in this study). The first part of this work presents a systematic review conducted on as-grown GaN substrates. The second part of this article focuses on H_3PO_4 and the related treatments were performed on both as-grown GaN and dry-etched GaN which are referred to as sample A and sample B respectively. The dry-etching process was an initial Inductive Coupled Plasma Reactive Ion Etching (ICP-RIE) plasma based on Cl_2/BCl_3 chemistry. The ICP-RIE was performed at low pressures, medium Transformer Coupled Plasma (TCP) powers, and at high bias voltage of 237 V. The ICP-RIE was followed by an Atomic Layer Etching (ALE) including a first chlorinated step Cl_2/BCl_3-based plasma at high pressure (50-100 mTorr), and no applied bias voltage, in order to encourage the chemical adsorption against ion formation and sputtering. The second step of the ALE was an Ar plasma at low pressures (5-20 mTorr) and a low applied bias (<70 V) in order to enhance the physical etching. The electrostatic chuck temperature was maintained under 80°C. Each steps were 5 seconds long and were separated by a purge step of several seconds. Finally, a stripping sequence was performed after the ICP-RIE and ALE steps in order to remove eventual etching by-products. It was composed of an O_2-based plasma succeeded by a wet treatment by a wet treatment with Dupont™ PlasmaSolv® EKC265™, a photoresist remover.

We examined the effect of several chemical treatments commonly encountered in the microelectronic industry: H_2SO_4 98%, HCl 37%, $(NH_4)_2S$ 26%, NH_4OH 27%, $(NH_4)_2S_2O_8$ (ammonium persulfate), H_3PO_4 85% and Caro acid 3:1 (H_2SO_4:H_2O_2). Additionally, 1M citric acid was tested. Unless specified otherwise, all treatments were performed at room temperature (RT).

After each treatment, samples were immediately transferred into a specific vacuum carrier (10^{-5} mbar) for surface analysis by pAR-XPS. The time between treatment and loading into the vacuum carrier did not exceed 20 minutes.

pAR-XPS measurements were performed using a customised Thermo Fisher Scientific Theta 300. X-rays were produced from a monochromatic Al-Kα anode source at 1486 eV, with a beam diameter on the sample of 400 µm and the analyses were performed under Ultra High Vacuum (UHV) (10^{-9} mbar). The use of pAR-XPS allows the collection of photo-emitted electrons at several angles at the same time without tilting the substrate. Photo-emitted electrons were collected simultaneously at eight angles from 23.75° to 76.25° with respect to the substrate normal. This gave accurate depth resolved information and enabled us to estimate the oxide thickness on GaN using the method described in [19]. The oxide thickness estimation was extracted from the Ga 2p peak. In order to quantify the surface composition, data were acquired for Ga3d, N1s, O1s, C1s, Cl2p and P2p with a pass energy of 100 eV. A 76.25° grazing angle was used for the quantification of each element, using the same method as in [20] [21]. All binding energies were calibrated with respect to the binding energy of the C 1s peak that was set at 285 eV.

Surface topography was examined by AFM using a tapping mode Bruker Dimension FastScan tool and analysed with the Bruker Nanoscope Software.

3. Results and discussion

3.1. Systematic review of wet etchants at room temperature

The impact of several wet etchants on non-intentionally doped as-grown GaN samples was investigated by pAR-XPS in order to analyse the chemical states of the elements present on the surface. Samples were immersed for 10 minutes as for a previous study [22] in the chosen chemical then rinsed for 5 minutes in de-ionized water and dried under N_2. The influence of wet etchants was evaluated based on the relative atomic percentage (at .%) of different elements. We also estimated the oxide thickness using the varied angle acquisition based on the hypothesis that the major oxide present on the surface was β-Ga_2O_3.

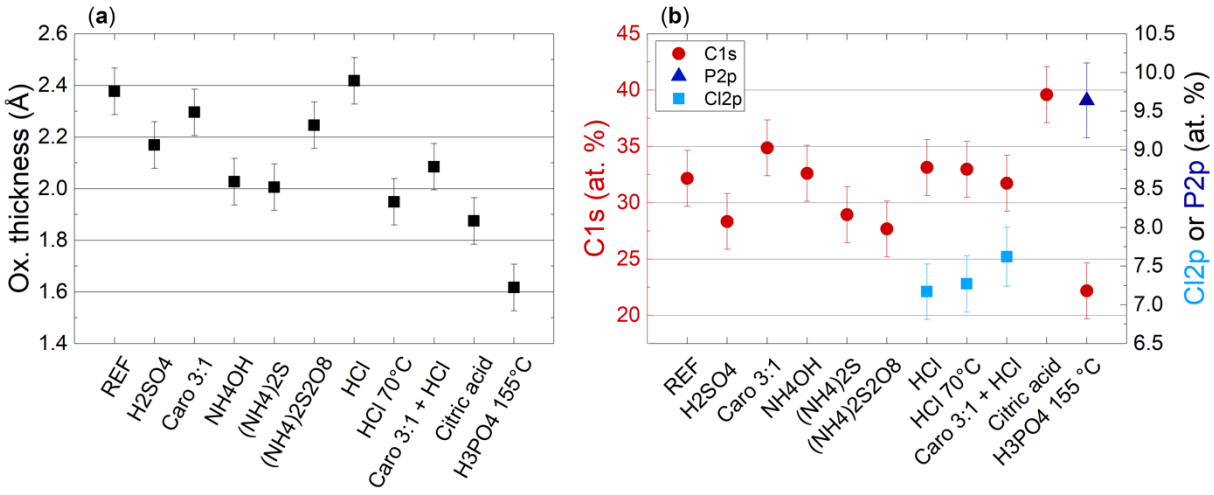


Figure 1. (a) Oxide thickness estimation on GaN by pAR-XPS after several wet treatments (10 min. immersion in the liquid etchants) and (b) atomic % of the total amount of C and Cl or P adsorbates on GaN induced by treatments. REF stands for as-grown GaN with a native oxide on top.

Fig. 1a shows the estimated oxide thickness for different chemicals. Oxidizing agents, such as pure sulphuric acid (H_2SO_4) or Caro (H_2SO_4:H_2O_2) solutions did not increase the oxide thickness. The H_2SO_4:H_2O_2 mixture was shown to induce hydroxyl oxide group adsorption [23]. It is commonly used to remove carbon contamination, although we see in Fig. 1b that the impact of Caro acid on carbon was negligible here (the carbon level is 32 at. % in the reference sample, vs 35 at. % after Caro treatment)

Basic chemicals such as NH_4OH and $(NH_4)_2S$ removed, as expected, some of the oxide from the surface (2.03 Å and 2.01 Å, respectively, versus 2.38 Å for the reference), in agreement with other results [24] [25] [26]. On the contrary, persulfate ammonium $(NH_4)_2S_2O_8$ had no significant impact on the oxygen level. Fig. 1b shows that sulphur-based treatments slightly reduced the amount of carbon while for other treatments, except citric acid, the quantity did not change. However, no peak related to the presence of sulphur was observed. One possible explanation might be that the sulphur level was below the detectability threshold.

There was otherwise a decrease of the oxide thickness for chlorine-based treatments, especially at 70°C and in combination with Caro 3:1. It is noteworthy that the same amount of chlorine was found (about 7 at. %) whatever the conditions, as shown is Fig. 1b. There is thus a strong possibility that chlorine atoms bond to Ga atoms, since the bond strength is higher for Ga-Cl than N-Cl [27]. Since

the chlorine level did not seem to depend on treatment conditions, the position of Cl atoms may have been different depending on the conditions, with a better oxidation prevention for hot HCl.

An interesting result is the decrease of oxide thickness after $C_6H_8O_7$ citric acid treatment (1.88 Å vs 2.38 Å for the reference). A slightly higher amount of oxygen (O 1s) was also found (19.4 at. % vs 18.7 at. % for the reference - see ESI Fig. S1). This can be attributed to the adsorption of citric acid, which brings both oxygen and carbon to the surface. This is backed up by the higher level of carbon found after citric acid treatment (39.6 at.% vs 32.0 at. % for the reference sample), as shown in Fig. 1b. Since the oxide thickness is lowered, it can be deduced that the adsorption of citric acid prevents oxidation. This result is in agreement with a previous work on Ge substrates [28].

Finally, the most important reduction of the oxide thickness was observed for the H_3PO_4 treatment at 155°C. We saw above that HCl-based treatments leave Cl on the surface. Similarly, P atoms were detected on the surface after immersion in H_3PO_4, as shown in Fig. 1b. At the same time, we also observed the lowest levels of carbon on GaN after a H_3PO_4 treatment.

This pAR-XPS systematic study is in agreement with previous works [25][27] . Results obtained here indicate that temperature seems to have an important role in reacting with the quasi-inert surface of c-plane Ga polarity GaN. In particular, we see that H_3PO_4, which has the highest boiling point of the chemical treatments, has the biggest impact on the oxide thickness.

Following these encouraging results, we examined the impact of H_3PO_4 on the GaN surface in more details in the next set of experiments.

3.2.Hot phosphoric acid treatment : influence of immersion duration

Among the existing high boiling point chemicals already used in the microelectronic industry, we have H_3PO_4 and KOH. One of the advantages of using H_3PO_4 for etching is the existence of specific equipment in order to maintain the water in the solution while heating it at high temperature. In addition, KOH is prohibited in many production fabs. This study therefore consisted of the immersion of the samples in H_3PO_4 for four different durations: 10, 20, 30 and 60 minutes.

We investigated two different GaN surfaces: as-grown and dry etched n-GaN samples. The dry etching process was an initial ICP-RIE followed by an ALE, a dry stripping sequence composed of an O_2-based plasma treatment and finally a dip in Dupont™ PlasmaSolv® EKC265™, a photoresist remover.

The Ga 3d spectra of these two surfaces were de-convoluted into two major contributions: Ga-N bonding, and, at higher binding energy, Ga-O bonding, as shown in Fig. 2. These components are 0.7 eV apart. It can be noticed that before H_3PO_4 treatment, the dry-etched sample does not exhibit a shift toward higher energy compared to the as-grown sample, unlike [29] [30]. It may be because after the plasmas the samples were dipped into EKC265™, which has an etchant effect, removing the oxides created by the plasmas. Indeed, EKC265™ contains hydroxylamine (NH_2-OH), which was reported to act as an etchant on AlN oxides [31].

After immersion in H_3PO_4, Ga 3d peaks shift toward higher binding energies, by about 0.7 eV and 0.5 eV for as-grown and dry etched samples, respectively. A shift toward higher binding energy typically reveals adsorption of oxygen in Ga-O^{2-} or Ga-OH^- forms [32] [33]. A shift toward higher binding energy of O 1s is also observed, as well as an intensity increase around 533 eV (not shown here), which is related to the presence of OH^- groups [15] [34]. Furthermore, a clear increase of the Ga-O component area can be noted when the samples are immersed for 30 and 60 minutes in H_3PO_4.

However, no change in the Ga-O component is observed after 10 and 20 minutes. The contribution in percent of each component is shown in Fig. 3 (a). A difference is seen between as-grown GaN and etched GaN. Indeed, dry etched samples are slightly more oxidised than as-grown samples, in line with previous work [35]. Next, we can see from Fig. 3 (a) that the Ga-O amount difference between dry-etched and as-grown samples is reduced after H_3PO_4 treatment and is likely due to damage removal from the dry-etched surface. We assume that the dry-etched GaN has initially more active sites that might be related to dangling bonds and vacancies to enable the formation of Ga-O bonds, while for the as-grown GaN fewer active sites were initially present. However, the number of active sites significantly increased between 30 and 60 minutes. Indeed, between 30 and 60 minutes of treatment, the as-grown sample otherwise gains almost 10 % in terms of Ga-O contribution whereas the dry etched sample barely gains 3 %. This means that after 60 minutes, they both have nearly 70% of Ga-O.

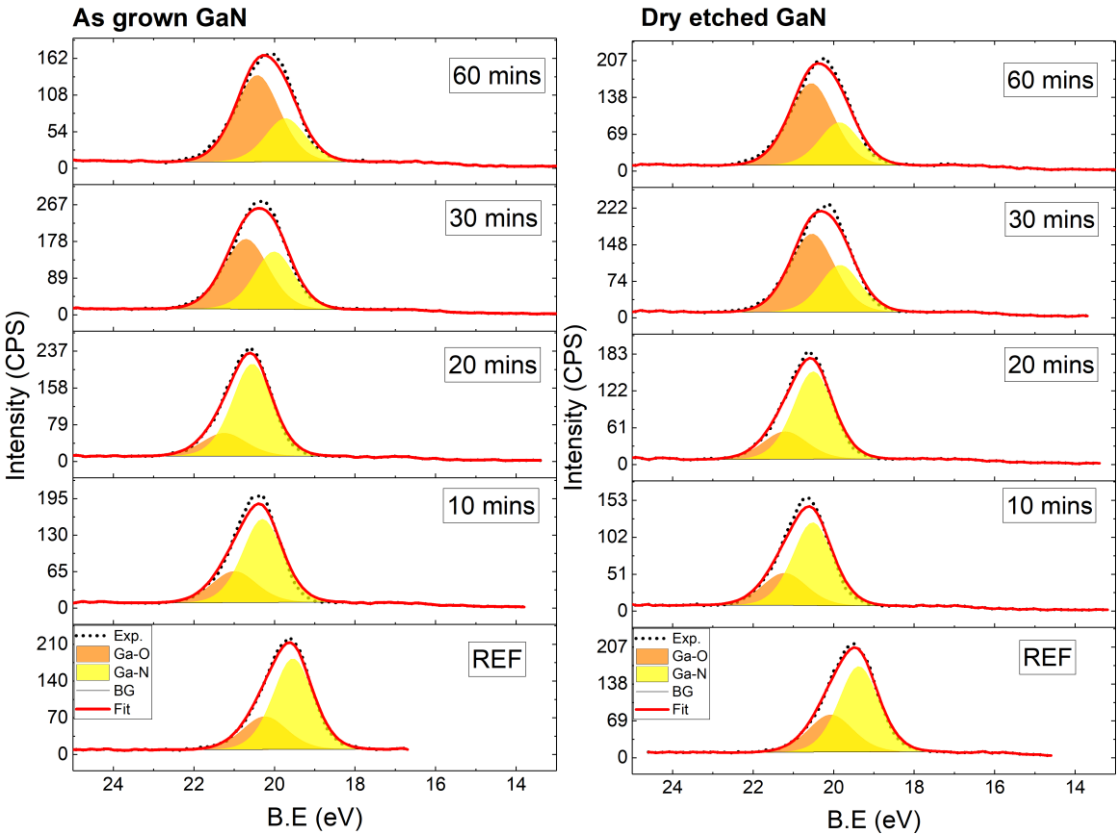


Figure 2. Evolution of the Ga 3d spectra of (left) as-grown GaN and (right) dry etched GaN at different times of H_3PO_4 treatment

The evolution of the estimated oxide thickness as a function of the immersion duration in H_3PO_4 (Fig. 3 (b)) follows the same evolution observed for the Ga-O contribution of the Ga 3d peak between 10 and 20 minutes for the as dry-etched GaN. However, morphological changes starting after 10 minutes for the as-grown GaN, which will be discussed later, may lead to errors in the estimation of the oxide thickness. The same remarks could be observed starting from 30 minutes for the dry-etched GaN. Indeed, the model does not fit after 30 minutes in H_3PO_4.

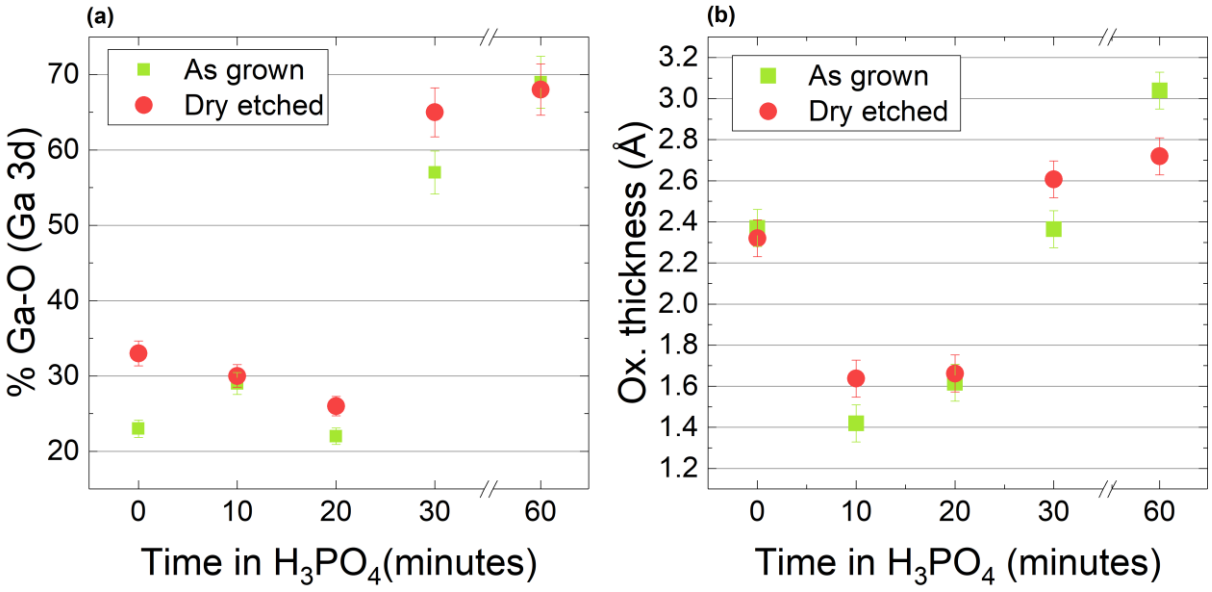


Figure 3. Evolution of (a) the Ga-O component from Ga 3d and (b) the estimated oxide thickness as a function of time in H_3PO_4

The observation of the N 1s spectra (Fig. 4) leads to a similar conclusion. After deconvolution, there is an increase of a component located around 398.9 eV. This component corresponds to nitrogen atoms for which their nearest neighbour has been replaced by oxygen [36] and is assigned as "N-Ga-O" on the spectra. As for Ga-O in the Ga 3d spectra, N-Ga-O started to increase after 30 minutes of treatment and further increased with the H_3PO_4 treatment duration.

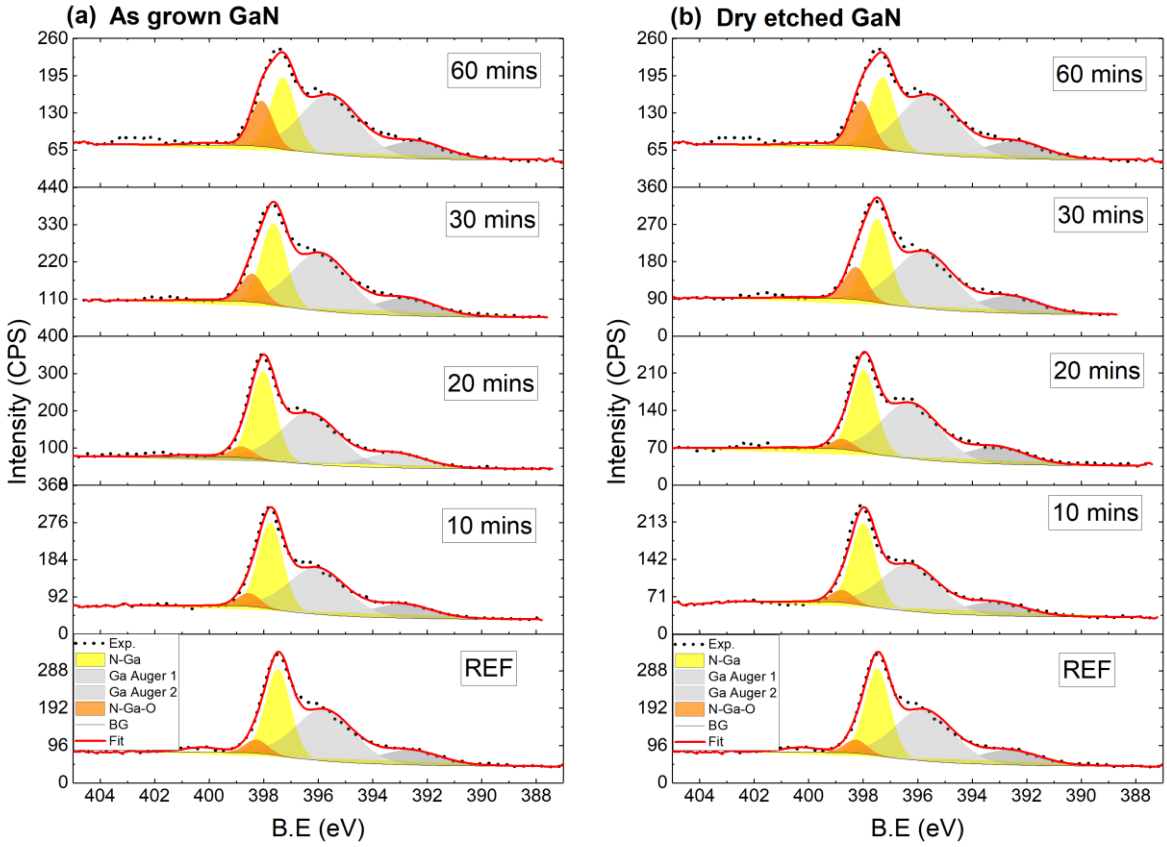


Figure 4. Evolution of the N 1s spectra of As-grown GaN (left) and dry etched GaN (right) at different times of treatment in H_3PO_4

The relative atomic percentage data for various elements on the surface of dry etched and as-grown samples are presented in tables S1 and S2 of the ESI, respectively. The total oxygen level was found to be the same before and after H_3PO_4 treatment and does not seem to be dependent on the immersion duration. The Ga 3d spectra show that immersion of GaN in H_3PO_4 has an impact on the bonding states of oxygen atoms. Dangling bonds might have been created, promoting thereby the increase of Ga-O bonds. The (0001) surface is very stable so the H_3PO_4 is not expected to attack everywhere. It is more likely that the attack occurs at non-equilibrium positions such as dislocations, atomic step edges, or surface defects.

Fig. 5 shows the Ga/N ratio, which was calculated based on the Ga-N components of Ga 3d and N 1s. A decrease is observed after 30 minutes of H_3PO_4 treatment for both surfaces. This result reveals a non-stoichiometric distribution of the gallium and nitrogen atoms at the surface, which was initially not far from Ga/N = 0.5. After 30 minutes of treatment, the Ga/N ratio reached 0.40 and 0.35 for the as-grown GaN and the dry-etched GaN respectively. While the ratio does not evolve after 60 minutes for the dry-etched GaN, it reduces to 0.37 for the as-grown GaN. Therefore, the Ga-N bonds at the surface are dissociated by the PO species in line with *Shintani et. al*. [38].

The surface, which is initially covered by the native oxide, is attacked at active sites, as suggested by [38] by the PO_4^{3-} dissociating the Ga-N bonds. Note that the exact nature of the Ga-POx bonds are unknown.

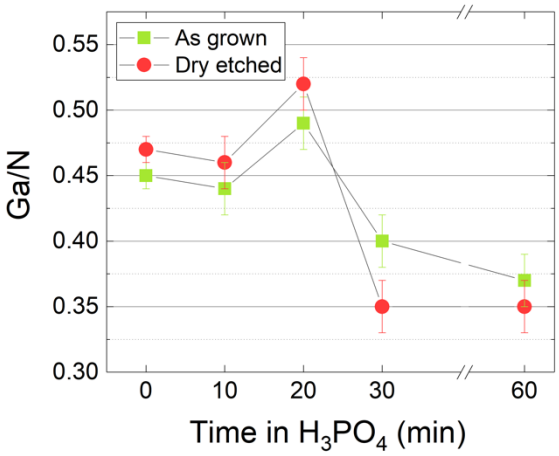


Figure 5. Evolution of the Ga/N surface ratio on as grown and dry etched GaN as a function of time in H_3PO_4

Morphological changes on as-grown and etched surfaces were examined by AFM. We see in Fig. 6 that, prior to H_3PO_4 treatment, the as-grown sample shows clearly defined rounded atomic steps, together with dark spots associated with threading dislocations having a screw type component. For the dry etched sample, the surface is rougher because of the plasma treatment. It is difficult to clearly see atomic steps and dislocations, then.

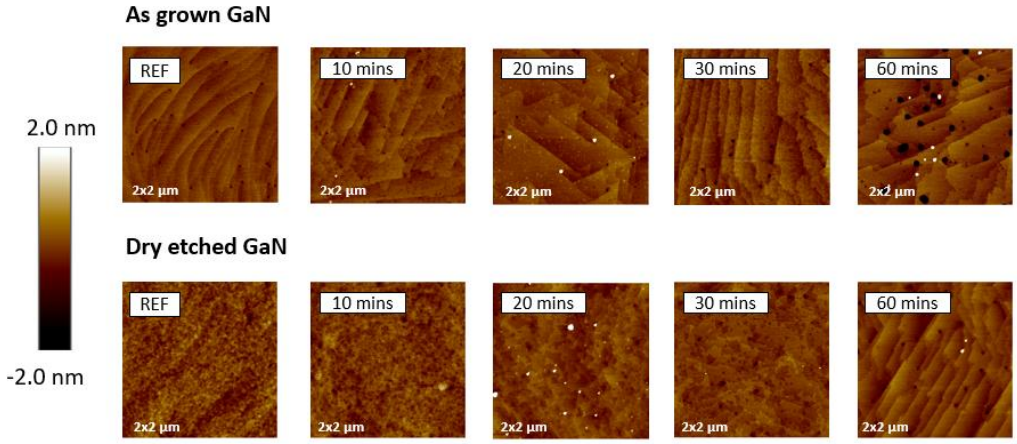


Figure 6. AFM images before and after hot H_3PO_4 treatment at different durations

For the as-grown sample, the atomic steps become straight and crystallographically aligned after a 10 minute immersion in H_3PO_4. After 20 minutes, steps start to become triangular. They become parallel after 30 minutes of immersion. Dark spots associated with threading dislocations on the as-grown sample become well defined hexagonal pits after 60 minutes in hot H_3PO_4 in line with literature results on c-plane GaN [4] [15] [39] [40]. In this case, there are two families of pits, one with diameters around 90 nm, another with diameters around 34 nm. There are 22 large pits after 60 minutes, compared with 21 pits on the surface of the as-grown sample without H_3PO_4 treatment. Larger holes might be the emergence points of dislocations with a screw component, while smaller ones are pure edge type. The total density of threading dislocations is therefore 1.9×10^9 cm^{-2}, in line with observations by *Yon et al.* [41] on similar samples. However, it is important to note that after 60 minutes, some of the large holes have hexagonal structures of different sizes, which is likely due to their overlapping making an accurate counting of dislocations difficult (Fig. 7).

These AFM results indicate that etchant species attack at defect points, i.e. dislocations or surface defects, in agreement with [42]. Etching is reported to be dependent on the number of dangling bonds on the surface [34]. This is shown by the opening of dislocations on inclined planes, with therefore different crystalline orientations on the surface. Atomic steps become aligned and straighter, in order to reduce their energy. This evolution is shown schematically in Figure 8.

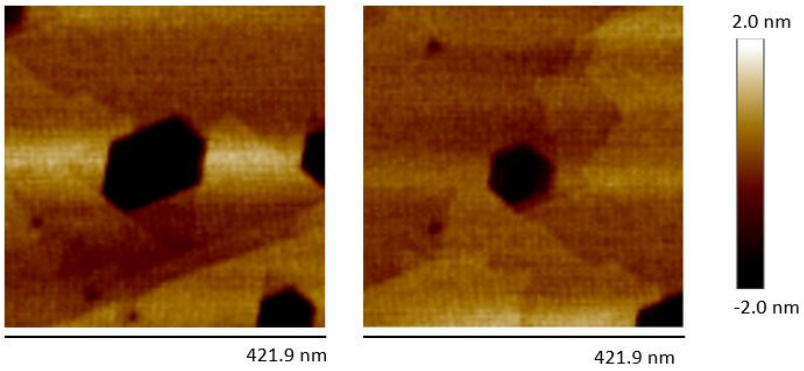


Figure 7. AFM images of overlapping dislocations (left) and of a single dislocation (right) of the surface of an as-grown sample after 60 minutes in H_3PO_4

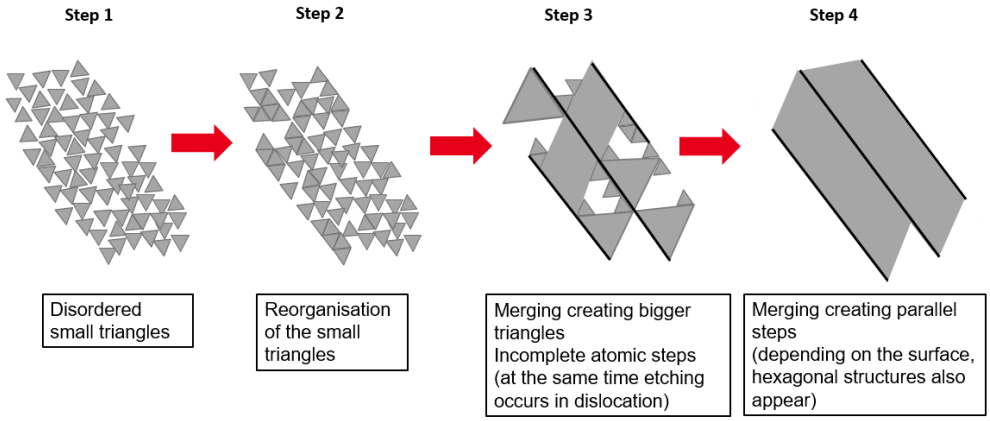


Figure 8. Evolution of the GaN surface for different durations in H_3PO_4. The fat black line is a visual guide to delimit the atomic steps

Based on these observations, we can thus suggest the following dry etched surface recovery mechanism upon immersion in H_3PO_4. The use of a plasma treatment results in an amorphous surface where surface defects are not directly accessible. The kinetic migration of the wet etchant species toward active sites is therefore decreased. The H_3PO_4 wet etching starts first with the removal of the amorphous layer caused by the dry etching. Next, the re-organisation of the surface starts, with the emergence of small triangular structures (Fig. 8, step 1). Small triangles merge overtime (Fig. 8, steps 2 and 3) leading to the appearance of parallel atomic steps oriented along the same crystallographic direction (Fig. 8, step 4), as seen for the as-grown sample. During that stage, there is a progressive revelation of dislocations. Finally, based on the AFM image of the as-grown sample (Fig. 6, top line), it is likely that dislocations will be further opened on GaN dry-etched surfaces for immersions longer than 60 minutes, with the same dislocations opening and merging [4].

3.3. Effect of ALE within the dry etching processes

Having shown that H_3PO_4 is able to recreate atomic steps and recover an excellent surface morphology on etched samples, we investigated its impact on dry etched GaN with and without the use of ALE (see table 1). Our aim was to better understand the role played by H_3PO_4 on defects and determine whether or not we could avoid using, thanks to its use, expensive and time-consuming ALE.

	Etching steps prior to H_3PO_4		
	ICP-RIE	ALE	Stripping sequence
Sample A			
Sample B	✓	✓	✓
Sample C	✓		✓

Table 1. Different etch treatments applied to different samples prior to H_3PO_4 wet etching.

Samples were immersed in H_3PO_4 for 30 minutes. This duration was chosen because it had an impact on the surface chemistry and did not result in any major degradation (wide dislocation opening) of the morphology of as-grown or dry etched samples. Ga 3d spectra before and after H_3PO_4 treatment are shown in Figure 9. The Ga 3d spectra of the sample C with "ICP-RIE+ stripping", i.e. without ALE, does not exhibit the same evolution as the "standard dry etch" sample B or the as-grown sample A. Indeed, no increase of the Ga-O component occurs. As stated before, the ICP-RIE process induces considerable damage such as the creation of dangling bonds and vacancies, making the surface somewhat amorphous. These induced defects can be found deep within the material. The subsequent ALE step removes the amorphous material, resulting in a lattice more similar to that of the as-grown sample. In contrast, the surface of sample C, which is directly exposed to an oxidative atmosphere right after the ICP-RIE etch, probably exhibits a more damaged surface with the incorporation of oxygen, weakening the Ga-N bonds even more. As a consequence, H_3PO_4 acts as an etchant with some oxide removal. The morphology of these samples was investigated by AFM before and after H_3PO_4. Images are shown in Figure 10. The final morphology of the surface of sample C after H_3PO_4 strongly differs from that of sample B with the "standard dry etching" process including ALE.

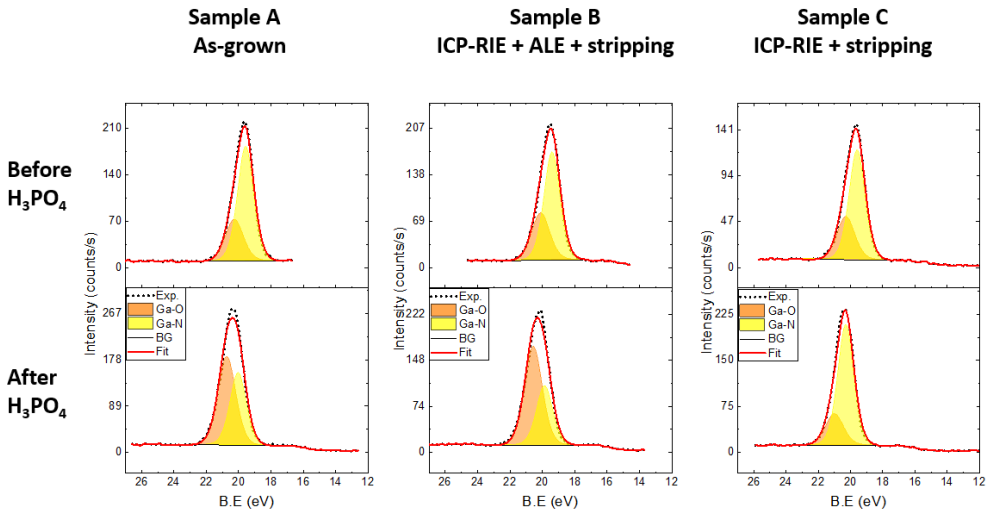


Figure 9. Evolution of the Ga 3d XPS spectra for samples A to C before and after 30 minutes of H_3PO_4 treatment

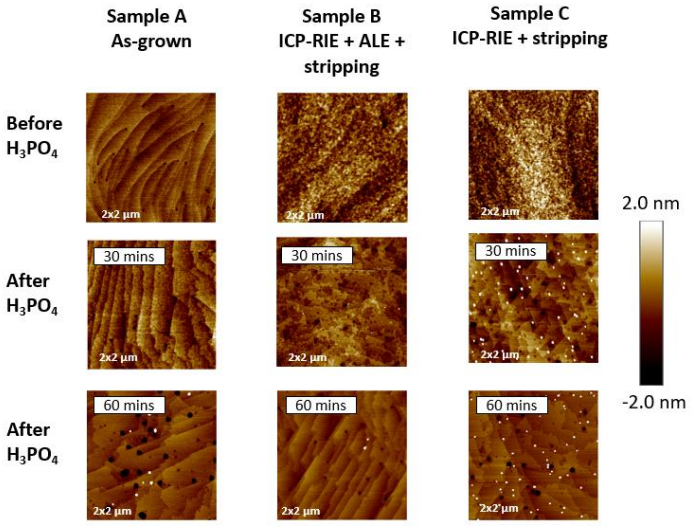


Figure 10. AFM images of the surface of samples A to C before and after 30 and 60 minutes of H_3PO_4 etching of the samples A to C

Sample C without ALE has a more organised surface after H_3PO_4 treatment. As seen in Figure 10, well-defined triangular structures appear after immersion of sample C into H_3PO_4, whereas triangular structures of the "standard dry etching" process (sample B) are less distinguishable and smaller.

We can thus assume that, after 30 minutes in H_3PO_4, sample C is at the second step of the etching scenario shown in Figure 8, with well-defined triangular structures. Meanwhile, sample B is at the first step, since its surface seems to be less organised with smaller triangular structures. Therefore, the delayed effect observed on dry etched samples B and C strongly depends on the steps following the ICP-RIE process. These observations are consistent with the report of *Tautz et al* [43] who reviewed the influence of surface damages induced by pre-processing on the etching rate of KOH. In our case, the ALE step seems to have a good effect on recovering the surface has less pits are visible on Sample B compared to Sample C after 30 minutes in H_3PO_4. Indeed, after 60 minutes of treatment the Sample B exhibited a recovery of the step edges whereas it is not the case for Sample C.

Despite these differences, AFM and XPS observations do not show the same evolution for all processes. There thus does seem to be a direct link between surface chemistry and morphology.

Finally, we should note that after a treatment with H_3PO_4, the residual P atoms might influence the devices properties by bringing charged species to the surface. However, at this time, it is unclear how this would affect the electrical properties, nor how detrimental their presence would be over time. Furthermore, during the device fabrication, the residual P atoms may desorb after the additional process steps required to fabricate the final device. This would be an important point to analyse with electrical tests after device fabrication.

4. Conclusions

Our systematic review of several etchants commonly encountered in the microelectronic industry revealed little modification in the surface of c-plane GaN, showing that the behaviour of GaN on silicon is coherent with the different sources of GaN in the literature. A detailed study by pAR-XPS showed that HCl, $(NH_4)_2S$, NH_4OH, citric acid and H_3PO_4 etched the surface oxide on GaN, with H_3PO_4 having the highest impact.

We thus investigated the impact of different immersion duration in hot H_3PO_4 on as-grown and dry etched GaN samples. Significant surface chemistry and morphology changes were seen for immersion durations of 30 minutes or more. These treatments enabled us to recover the atomic steps on as-grown and dry-etched GaN surfaces, although this recovery was delayed on dry etched GaN surfaces. This was probably due to the time required to remove the surface layers damaged by dry etching. We also studied the impact of ALE in the overall dry etching sequence. This step also modified the delay time, with different impacts on the chemistry of the surface and its morphology. Surface damage right after the use of a standard ICP-RIE dry etching process most likely had a role.

We showed here that an immersion in H_3PO_4 is a promising treatment to recover a high quality GaN surface after various types of dry etchings. In contrast to other studies, we have shown that, with a controlled environment, it is possible to recreate atomic steps on a GaN surface without significantly opening dislocation holes. This is therefore a treatment which would be applicable to recessed gate HEMT processing to recover surfaces after GaN dry etching.

Electrical characterisation will shortly be performed to determine the beneficial or detrimental re-organisation of the surface and/or the presence of POx species.

Acknowledgments

This work has been partially supported by the French Government Program “Investissements d’Avenir” managed by the National Research Agency (ANR) under the contract number ANR-10-EQPX-33 and by the French RENATECH network

References

[1] M. Su, C. Chen, et S. Rajan, « Prospects for the application of GaN power devices in hybrid electric vehicle drive systems », *Semicond. Sci. Technol.*, vol. 28, n° 7, p. 074012, juin 2013, doi: 10.1088/0268-1242/28/7/074012.

[2] M. Charles *et al.*, « (Invited) Epitaxy of GaN on Si (111) for Power Electronics, RF and LEDs », *ECS Trans.*, vol. 86, n° 7, p. 233, juill. 2018, doi: 10.1149/08607.0233ecst.

[3] L. Liu et J. H. Edgar, « Substrates for gallium nitride epitaxy », *Mater. Sci. Eng. R Rep.*, vol. 37, n° 3, p. 61‑127, avr. 2002, doi: 10.1016/S0927-796X(02)00008-6.

[4] S.-C. Han *et al.*, « Formation of Hexagonal Pyramids and Pits on V-/VI-Polar and III-/II-Polar GaN/ZnO Surfaces by Wet Etching », *J. Electrochem. Soc.*, vol. 157, n° 1, p. D60, 2010, doi: 10.1149/1.3253564.

[5] E. A. Jones, F. F. Wang, et D. Costinett, « Review of Commercial GaN Power Devices and GaN-Based Converter Design Challenges », *IEEE J. Emerg. Sel. Top. Power Electron.*, vol. 4, n° 3, p. 707‑719, sept. 2016, doi: 10.1109/JESTPE.2016.2582685.

[6] R. J. Shul *et al.*, « Inductively coupled high-density plasma-induced etch damage of GaN MESFETs », *Solid-State Electron.*, vol. 45, n° 1, p. 13‑17, janv. 2001, doi: 10.1016/S0038-1101(00)00164-7.

[7] C. R. Eddy et B. Molnar, « Plasma etch-induced conduction changes in gallium nitride », *J. Electron. Mater.*, vol. 28, n° 3, p. 314‑318, mars 1999, doi: 10.1007/s11664-999-0033-y.

[8] H. Tokuda, S. Harada, J. T. Asubar, et M. Kuzuhara, « Influence of reactive-ion-etching depth on interface properties in Al2O3/n-GaN MOS diodes », *Jpn. J. Appl. Phys.*, vol. 58, n° 10, p. 106503, sept. 2019, doi: 10.7567/1347-4065/ab3d11.
[9] Y. Jiang *et al.*, « GaN MOSFET with Boron Trichloride-Based Dry Recess Process », *J. Phys. Conf. Ser.*, vol. 441, p. 012025, juin 2013, doi: 10.1088/1742-6596/441/1/012025.
[10] J.-M. Lee, K.-M. Chang, S.-W. Kim, C. Huh, I.-H. Lee, et S.-J. Park, « Dry etch damage in *n* -type GaN and its recovery by treatment with an N2 plasma », *J. Appl. Phys.*, vol. 87, n° 11, p. 7667‑ 7670, juin 2000, doi: 10.1063/1.373438.
[11] S. Ruel *et al.*, « Atomic layer etching of GaN using Cl2 and He or Ar plasma », *J. Vac. Sci. Technol. A*, vol. 39, n° 2, p. 022601, févr. 2021, doi: 10.1116/6.0000830.
[12] L. Wang, Y. Bu, et J.-P. Ao, « Effect of oxygen plasma treatment on the performance of AlGaN/GaN ion-sensitive field-effect transistors », *Diam. Relat. Mater.*, vol. 73, p. 1‑ 6, mars 2017, doi: 10.1016/j.diamond.2016.11.002.
[13] A. Yamamoto, K. Kanatani, S. Makino, et M. Kuzuhara, « Metalorganic vapor phase epitaxial growth of AlGaN directly on reactive-ion etching-treated GaN surfaces to prepare AlGaN/GaN heterostructures with high electron mobility ($\sim$1500 cm ^{2} V $^{-1}$ s $^{-1}$): Impacts of reactive-ion etching-damaged layer removal », *Jpn. J. Appl. Phys.*, vol. 57, n° 12, p. 125501, déc. 2018, doi: 10.7567/JJAP.57.125501.
[14] C. B. Vartuli *et al.*, « Wet chemical etching survey of III-nitrides », *Solid-State Electron.*, vol. 41, n° 12, p. 1947‑ 1951, déc. 1997, doi: 10.1016/S0038-1101(97)00173-1.
[15] M. Mishra *et al.*, « Wet chemical etching induced stress relaxed nanostructures on polar & non-polar epitaxial GaN films », *Phys. Chem. Chem. Phys.*, vol. 19, n° 13, p. 8787‑ 8801, mars 2017, doi: 10.1039/C7CP00380C.
[16] S. J. Wilkins, T. Paskova, et A. Ivanisevic, « Effect of etching with cysteamine assisted phosphoric acid on gallium nitride surface oxide formation », *J. Appl. Phys.*, vol. 114, n° 6, p. 064907, août 2013, doi: 10.1063/1.4817899.
[17] X. Xu, R. P. Vaudo, J. Flynn, et G. R. Brandes, « Acid etching for accurate determination of dislocation density in GaN », *J. Electron. Mater.*, vol. 31, n° 5, p. 402‑ 405, mai 2002, doi: 10.1007/s11664-002-0091-x.
[18] M. Charles *et al.*, « The effect of AlN nucleation temperature on inverted pyramid defects in GaN layers grown on 200mm silicon wafers », *J. Cryst. Growth*, vol. 464, p. 164‑ 167, avr. 2017, doi: 10.1016/j.jcrysgro.2016.11.049.
[19] M. Legallais *et al.*, « Improvement of AlN Film Quality Using Plasma Enhanced Atomic Layer Deposition with Substrate Biasing », *ACS Appl. Mater. Interfaces*, vol. 12, n° 35, p. 39870‑ 39880, sept. 2020, doi: 10.1021/acsami.0c10515.
[20] M. A. Mahjoub *et al.*, « Impact of wet treatments on the electrical performance of Ge0.9Sn0.1 based p-MOS capacitors », p. 27.
[21] T. Haffner *et al.*, « Improvement of the electrical performance of Au/Ti/HfO_2/$Ge_{0.9}Sn_{0.1}$ p-MOS capacitors by using interfacial layers », *Appl. Phys. Lett.*, vol. 115, n° 17, p. 171601, oct. 2019, doi: 10.1063/1.5121474.
[22] R. Meunier *et al.*, « XPS Analysis of AlGaN/GaN Surface after Chemical and N-Containing Plasma Treatments », *ECS Trans.*, vol. 50, n° 3, p. 451‑ 460, mars 2013, doi: 10.1149/05003.0451ecst.
[23] H. Wang, H. Zhang, J. Liu, D. Xue, H. Liang, et X. Xia, « Hydroxyl Group Adsorption on GaN (0001) Surface: First Principles and XPS Studies », *J. Electron. Mater.*, vol. 48, n° 4, p. 2430‑ 2437, avr. 2019, doi: 10.1007/s11664-019-07011-1.

[24] K. Prabhakaran, T. G. Andersson, et K. Nozawa, « Nature of native oxide on GaN surface and its reaction with Al », *Appl. Phys. Lett.*, vol. 69, n° 21, p. 3212‑ 3214, nov. 1996, doi: 10.1063/1.117964.
[25] M. Diale, F. D. Auret, N. G. van der Berg, R. Q. Odendaal, et W. D. Roos, « Analysis of GaN cleaning procedures », *Appl. Surf. Sci.*, vol. 246, n° 1‑ 3, p. 279‑ 289, juin 2005, doi: 10.1016/j.apsusc.2004.11.024.
[26] T. Maruyama *et al.*, « Surface treatment of GaN and InN using (NH4)2Sx », *Phys. Status Solidi C*, vol. 0, n° 7, p. 2031‑ 2034, déc. 2003, doi: 10.1002/pssc.200303489.
[27] S. W. King *et al.*, « Cleaning of AlN and GaN surfaces », *J. Appl. Phys.*, vol. 84, n° 9, p. 5248‑ 5260, nov. 1998, doi: 10.1063/1.368814.
[28] T. Alphazan *et al.*, « Shallow Heavily Doped n++ Germanium by Organo-Antimony Monolayer Doping », *ACS Appl. Mater. Interfaces*, vol. 9, n° 23, p. 20179‑ 20187, juin 2017, doi: 10.1021/acsami.7b02645.
[29] Y. Zhong, « Self-terminated etching of GaN with a high selectivity over AlGaN under inductively coupled Cl2/N2/O2 plasma with a low-energy ion bombardment », *Appl. Surf. Sci.*, p. 8, 2017.
[30] M. Grodzicki, P. Mazur, et A. Ciszewski, « Changes of electronic properties of p-GaN(0 0 0 1) surface after low-energy N+-ion bombardment », *Appl. Surf. Sci.*, vol. 440, p. 547‑ 552, mai 2018, doi: 10.1016/j.apsusc.2018.01.097.
[31] A. Constant *et al.*, « Selective wet etching and hydrolysis of polycrystalline AlN films grown by metal organic chemical vapor deposition », *Mater. Sci. Semicond. Process.*, vol. 137, p. 106157, janv. 2022, doi: 10.1016/j.mssp.2021.106157.
[32] V. M. Bermudez, « Study of oxygen chemisorption on the GaN(0001)-(1×1) surface », *J. Appl. Phys.*, vol. 80, n° 2, p. 1190‑ 1200, juill. 1996, doi: 10.1063/1.362924.
[33] B. S. Eller, J. Yang, et R. J. Nemanich, « Electronic surface and dielectric interface states on GaN and AlGaN », *J. Vac. Sci. Technol. Vac. Surf. Films*, vol. 31, n° 5, p. 050807, sept. 2013, doi: 10.1116/1.4807904.
[34] D. Li *et al.*, « Selective etching of GaN polar surface in potassium hydroxide solution studied by x-ray photoelectron spectroscopy », *J. Appl. Phys.*, vol. 90, n° 8, p. 4219‑ 4223, oct. 2001, doi: 10.1063/1.1402966.
[35] L. Vauche *et al.*, « Study of an Al_2O_3 /GaN Interface for Normally Off MOS-Channel High-Electron-Mobility Transistors Using XPS Characterization: The Impact of Wet Surface Treatment on Threshold Voltage V_{TH} », *ACS Appl. Electron. Mater.*, vol. 3, n° 3, p. 1170‑ 1177, mars 2021, doi: 10.1021/acsaelm.0c01023.
[36] H. M. Liao, R. N. S. Sodhi, et T. W. Coyle, « Surface composition of AlN powders studied by x-ray photoelectron spectroscopy and bremsstrahlung-excited Auger electron spectroscopy », *J. Vac. Sci. Technol. A*, vol. 11, n° 5, p. 2681‑ 2686, sept. 1993, doi: 10.1116/1.578626.
[37] S. J. Wilkins, T. Paskova, C. L. Reynolds, et A. Ivanisevic, « Comparison of the Stability of Functionalized GaN and GaP », *ChemPhysChem*, vol. 16, n° 8, p. 1687‑ 1694, 2015, doi: 10.1002/cphc.201500105.
[38] A. Shintani et S. Minagawa, « Etching of GaN Using Phosphoric Acid », *J. Electrochem. Soc.*, vol. 123, n° 5, p. 706‑ 713, 1979, doi: 10.1149/1.2132914.
[39] L. Ravi et B. Krishnan, « Epitaxial growth of AlN microwalls on wet etched GaN template by MOCVD », *Superlattices Microstruct.*, vol. 123, p. 144‑ 153, nov. 2018, doi: 10.1016/j.spmi.2018.07.011.

[40] S. K. Hong, B. J. Kim, H. S. Park, Y. Park, S. Y. Yoon, et T. I. Kim, « Evaluation of nanopipes in MOCVD grown (0001) GaN/Al2O3 by wet chemical etching », *J. Cryst. Growth*, vol. 191, n° 1‑ 2, p. 275‑ 278, juill. 1998, doi: 10.1016/S0022-0248(98)00366-2.
[41] V. Yon, N. Rochat, M. Charles, E. Nolot, et P. Gergaud, « X-Ray Diffraction Microstrain Analysis for Extraction of Threading Dislocation Density of GaN Films Grown on Silicon, Sapphire, and SiC Substrates », *Phys. Status Solidi B*, vol. 257, n° 4, p. 1900579, 2020, doi: https://doi.org/10.1002/pssb.201900579.
[42] P. Visconti *et al.*, « Investigation of defects and surface polarity in GaN using hot wet etching together with microscopy and diffraction techniques », *Mater. Sci. Eng. B*, vol. 93, n° 1, p. 229‑ 233, mai 2002, doi: 10.1016/S0921-5107(02)00011-9.
[43] M. Tautz et D. Díaz Díaz, « Wet-Chemical Etching of GaN: Underlying Mechanism of a Key Step in Blue and White LED Production », *ChemistrySelect*, vol. 3, n° 5, p. 1480‑ 1494, 2018, doi: https://doi.org/10.1002/slct.201702267.